J. Ris. & Ap. Mat. Vol. 10, No. 2 (2026), pp. 333–350.
Jurnal Riset dan Aplikasi Matematika (JRAM)
e-ISSN: 2581-0154
DOI: doi.org/10.26740/jram.v10n2.p333-350

CAPUTO FRACTIONAL DERIVATIVE MODELING FOR THE SPREAD OF JAPANESE ENCEPHALITIS USING THE ADAMS–BASHFORTH–MOULTON METHOD

Drestanta Pambudi, Hairur Rahman*, and Dian Maharani

Mathematics Study Program, UIN Maulana Malik Ibrahim Malang, Indonesia

Corresponding Author: hairur@mat.uin-malang.ac.id

ABSTRACT

Japanese encephalitis (JE) is a mosquito-borne viral disease involving complex transmission dynamics among mosquitoes and vertebrate hosts, with pigs acting as amplifying hosts and humans generally considered dead-end hosts. This study develops an eleven-compartment fractional-order mathematical model of JE transmission involving human, pig, and mosquito populations using the Caputo fractional derivative. The model explicitly incorporates human vaccination, disease progression, pig infection and recovery, and exposed and infectious mosquito compartments. The mathematical analysis addresses the existence and uniqueness of solutions, positive invariance, the disease-free equilibrium, the basic reproduction number, stability, and sensitivity analysis. Numerical solutions are obtained using the Adams–Bashforth–Moulton (ABM) predictor–corrector method for fractional orders $\alpha = 1.00$, 0.90, 0.85, *and* 0.75. *The simulations show that decreasing the fractional order is associated with lower and later infection peaks in human and mosquito populations, followed by more prolonged declines. In the pig population, lower fractional orders produce a more gradual decline in the infectious population. Additional simulations show that increasing the human vaccination rate accelerates the decline of the susceptible human population, while variations in the pig-to-mosquito transmission rate produce closely overlapping trajectories for the infectious pig population under the scenarios examined. Compared with an earlier Caputo fractional-order JE model, this study adopts a different compartmental structure and investigates the resulting infection dynamics using the ABM predictor–corrector method. The findings characterize the effects of fractional order and selected epidemiological parameters within the proposed model, providing a basis for examining JE transmission dynamics under alternative compartmental assumptions.*

Keywords: *Japanese encephalitis; Caputo fractional derivative; fractional-order epidemic model; Adams–Bashforth–Moulton method; human–pig–mosquito transmission.*

1. Introduction

Japanese encephalitis (JE) is a mosquito-borne viral disease caused by the Japanese encephalitis virus (JEV), which remains an important public health concern in Asia and the Western Pacific. According to the World Health Organization [1], approximately 100,000 clinical cases and 25,000 deaths occur globally each year, while 24 countries in the WHO South-East Asia and Western Pacific Regions face a risk of JEV transmission. The virus is transmitted by infected *Culex* mosquitoes and circulates among mosquitoes and vertebrate hosts, particularly pigs and water birds. Humans are generally considered dead-end hosts because the viraemia following infection is insufficient to infect feeding mosquitoes. Letson et al. [2] further discussed the role of vaccination programmes in reducing JE incidence in endemic countries, although the magnitude

2020 Mathematics Subject Classification: 34A08, 92D30, 65L06
Received: 12-06-2026, revised: 27-10-2026, accepted: 30-10-2026.

of their impact varies with programme implementation and duration. These epidemiological characteristics highlight the importance of understanding interactions between mosquito vectors and vertebrate hosts when investigating JE transmission dynamics and developing mathematical models.

Mathematical modelling provides a framework for investigating JE transmission by representing interactions among humans, mosquitoes, and animal reservoirs. Baniya and Keval [3] developed a model incorporating human, pig, and mosquito populations to investigate the influence of vaccination on disease control. Ndaïrou, Area, and Torres [4] extended the modelling framework by considering aquatic environmental effects on mosquito population dynamics, while Sari, Andayani, and Wijaya [5] examined vector–reservoir transmission. Furthermore, Ladreyt et al. [6] investigated JE transmission in a rural Cambodian setting using a multi-host model calibrated with field data, highlighting the importance of host composition and ecological context in understanding human exposure. These studies demonstrate that mathematical models can be used to investigate disease-free equilibria, basic reproduction numbers, stability, and the effects of epidemiological parameters on transmission. They also indicate that model structure and biological assumptions influence the interpretation of transmission dynamics.

Most mathematical models of JE employ ordinary differential equations (ODEs), in which the rate of change of each epidemiological compartment is determined by the current state of the system. This approach has been used to investigate transmission dynamics, equilibrium points, stability, and control strategies, as demonstrated by Baniya and Keval [3] and Ndaïrou, Area, and Torres [4]. However, conventional integer-order models do not explicitly incorporate memory through a history-dependent derivative operator. Fractional-order differential equations offer an alternative framework in which the derivative can represent the influence of a system's past states on its subsequent evolution. This property may be relevant when investigating epidemiological processes involving temporal dependence. Nevertheless, fractional-order modelling should not automatically be considered more accurate than integer-order modelling; its suitability depends on the research question, biological assumptions, and available empirical evidence.

The Caputo fractional derivative is adopted in this study because it permits conventional initial conditions to be specified in terms of epidemiological state variables and provides a framework for examining history-dependent dynamics. Tuan et al. [7] investigated fractional differential equations using the Caputo operator and a generalized Adams–Bashforth–Moulton method, demonstrating the applicability of this numerical approach to fractional-order systems. Farooq et al. [8] examined a fractional vector–host disease model using Caputo and Atangana–Baleanu operators, while Akindeinde et al. [9] applied a Caputo-based fractional SEIRP model and the Adams–Bashforth–Moulton (ABM) method to COVID-19 transmission. These studies provide methodological context for the present work. In the JE setting, the fractional-order formulation enables the numerical trajectories of the epidemiological compartments to be compared across different fractional orders, including the integer-order limit as the fractional order approaches one. The use of a fractional derivative, however, does not by itself establish greater biological accuracy or predictive performance.

Previous studies have examined JE transmission from several complementary perspectives. Baniya and Keval [3] investigated vaccination in a model involving humans, pigs, and mosquitoes, whereas Ndaïrou, Area, and Torres [4] considered environmental effects on mosquito dynamics. Sari, Andayani, and Wijaya [5] analysed vector–reservoir transmission, while Ladreyt et al. [6] used field-calibrated modelling to investigate multi-host transmission and human exposure. Laidlow et al. [10] reviewed published JE transmission models and documented variation in model structures, population representation, and the use of empirical data. More specifically, Ghassabzade and Bagherpoorfard [11] developed a Caputo fractional-order

JE model and examined its mathematical properties, including the basic reproduction number and numerical solutions obtained using a product-integration method. Their study establishes that fractional calculus has already been applied to JE transmission modelling. Consequently, neither the application of the Caputo derivative to JE nor the use of fractional-order modelling alone can be claimed as the principal novelty of the present study.

The research gap addressed here concerns the formulation and analysis of a particular multi-population JE model and the numerical investigation of its dynamics under different fractional orders. The present model comprises eleven compartments representing human vaccination and disease progression, pig infection and recovery, and the susceptible, exposed, and infectious stages of mosquitoes. It explicitly adopts the biological assumptions that pigs act as amplifying hosts and humans are dead-end hosts. Compared with the fractional JE model developed by Ghassabzade and Bagherpoorfard [11], the present study employs a different compartmental representation and uses the ABM predictor–corrector method to investigate the resulting numerical dynamics. The contribution therefore lies in the specific combination of compartmental assumptions, mathematical analysis, and numerical investigation, rather than in claiming that fractional-order JE modelling has not previously been studied.

The contributions of this study are threefold. First, an eleven-compartment Caputo fractional-order model is formulated to represent transmission among human, pig, and mosquito populations, including human vaccination and the exposed stage of mosquitoes. Second, the mathematical properties of the model are investigated through the analysis of solution existence and uniqueness, positive invariance, the disease-free equilibrium, the basic reproduction number, stability, and parameter sensitivity. Third, numerical solutions are obtained using the ABM predictor–corrector method for fractional orders $\alpha \in \{1.00, 0.90, 0.85, 0.75\}$ to examine how changes in the fractional order affect the temporal trajectories of the epidemiological compartments. The numerical results indicate differences in infection peak timing, peak magnitude, and post-peak decline across the simulated populations. These findings characterize the behaviour of the proposed model under the selected parameter values and initial conditions without implying empirical validation against observed JE data.

Accordingly, the objective of this study is to formulate and analyse a fractional-order mathematical model describing JE transmission among human, pig, and mosquito populations using the Caputo fractional derivative. Specifically, the study examines the mathematical properties of the model, including solution existence and uniqueness, positive invariance, the disease-free equilibrium, the basic reproduction number, stability, and parameter sensitivity. It also applies the ABM predictor–corrector method to obtain numerical solutions and investigate the effects of varying the fractional order and selected epidemiological parameters on the resulting transmission dynamics. Through comparison with previous JE models, particularly the fractional-order model of Ghassabzade and Bagherpoorfard [11], this study seeks to clarify the contribution of its compartmental formulation and numerical analysis to the mathematical modelling of JE transmission.

2. Theoretical Background

This section presents definitions and theorems from fractional calculus used in this study. The main references are [12] and [13].

Definition 2.1 (Riemann–Liouville Fractional Derivative [12, 14])**.** *The Riemann–Liouville fractional derivative of order q of $f : (0, \infty) \to \mathbb{R}$ is*

$$ {}^{RL}D^{q} f(t) = \frac{1}{\Gamma(n-q)} \frac{d^n}{dt^n} \int_0^t (t-\tau)^{n-q-1} f(\tau)\, d\tau, $$

where $n - 1 < q \leq n$, $n \in \mathbb{Z}^+$, $t > 0$.

Definition 2.2 (Caputo Fractional Derivative [12, 14]). *Let $n-1 < q \leq n$ with $n \in \mathbb{N}$. The Caputo fractional derivative of order q of $f(t)$ is*

$$^{C}D^{q} f(t) = \frac{1}{\Gamma(n-q)} \int_0^t \frac{f^{(n)}(s)}{(t-s)^{q-n+1}}\, ds.$$

For $0 < q \leq 1$ this reduces to

$$^{C}D^{q} f(t) = \frac{1}{\Gamma(1-q)} \int_0^t (t-s)^{-q} f'(s)\, ds.$$

When $q \to 1$, the Caputo derivative coincides with the ordinary derivative: $^{C}D^{1} f(t) = f'(t)$.

Definition 2.3 (Caputo Fractional Integral [12, 14]). *The Caputo fractional integral of order q of $f(t)$ is*

$$I^{q} f(t) = \frac{1}{\Gamma(q)} \int_0^t (t-s)^{q-1} f(s)\, ds.$$

Definition 2.4 (Laplace Transform of the Caputo Operator [12, 14]).

$$\mathcal{L}[^{C}D^{q} y(t)](s) = s^{q}\mathcal{L}[y(t)] - \sum_{i=0}^{m-1} s^{q-i-1} y^{(i)}(0), \quad m-1 < q \leq m,\ m \in \mathbb{N}.$$

Definition 2.5 (Two-Parameter Mittag-Leffler Function [14]).

$$E_{\alpha,\beta}(z) = \sum_{k=0}^{\infty} \frac{z^{k}}{\Gamma(\alpha k + \beta)}, \quad \alpha, \beta > 0,\ z \in \mathbb{C}.$$

The Laplace transform of $t^{\beta-1} E_{\alpha,\beta}(\pm a t^{\alpha})$ is $s^{\alpha-\beta}/(s^{\alpha} \mp a)$.

Lemma 2.6 (Generalized Mean Value Theorem [15]). *Let $f \in C[a,b]$ and $^{C}D^{q} f \in C[a,b]$ for $q \in (0,1]$. Then there exists $\eta \in [a,t]$ such that*

$$f(t) = f(a) + \frac{^{C}D^{q} f(\eta)}{\Gamma(q+1)} (t-a)^{q}.$$

3. Research Method

This study modifies the SIR/SEIR model with additional assumptions to obtain a *Susceptible Vaccinated Exposed Infected Recovered* (SVEIRP) dynamical system model for three populations—human, pig, and mosquito—in ODE form. The model is then generalized to a fractional differential equation model by replacing d/dt with the Caputo derivative $^{C}D_{t}^{\alpha}$, followed by analysis and numerical solution using the ABM method. Model assumptions are:

1. All three populations have constant recruitment rates Λ_H, Λ_P, and Λ_M.
2. JEV is transmitted only via infected mosquito bites to humans or pigs; no direct human-to-human or pig-to-pig transmission occurs.
3. Pigs are the primary amplifying host: mosquitoes feeding on infectious pigs become exposed at rate β_{MP}.
4. Humans are dead-end hosts: mosquitoes biting infectious humans do not acquire JEV.

5. Susceptible humans (S_H) who are vaccinated move to V_H at rate ϕ_H and are fully protected from infection.
6. Infectious mosquitoes (I_M) do not recover and remain infectious until death.
7. Post-infection immunity in humans is permanent.
8. The fractional order α is identical for all eleven equations (*commensurate order*).

Based on these assumptions, the compartmental flow diagram is shown in Figure 1.

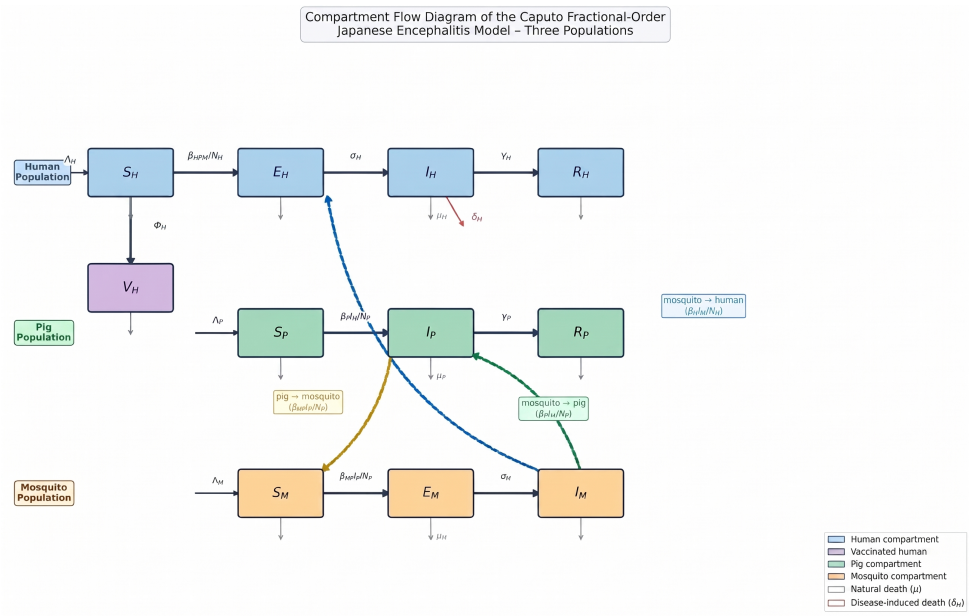


Figure 1. Compartmental flow diagram of the Caputo fractional JE model for three populations (human, pig, mosquito). Colored dashed arrows indicate cross-population transmission: blue (mosquito→human), green (mosquito→pig), yellow (pig→mosquito).

Based on this diagram, the dynamical system model is formulated as follows.

Human Population

$$\frac{dS_H}{dt} = \Lambda_H - \frac{\beta_H S_H I_M}{N_H} - (\phi_H + \mu_H)S_H, \tag{8}$$

$$\frac{dV_H}{dt} = \phi_H S_H - \mu_H V_H, \tag{9}$$

$$\frac{dE_H}{dt} = \frac{\beta_H S_H I_M}{N_H} - (\sigma_H + \mu_H)E_H, \tag{10}$$

$$\frac{dI_H}{dt} = \sigma_H E_H - (\gamma_H + \delta_H + \mu_H)I_H, \tag{11}$$

$$\frac{dR_H}{dt} = \gamma_H I_H - \mu_H R_H. \tag{12}$$

Pig Population

$$\frac{dS_P}{dt} = \Lambda_P - \frac{\beta_P S_P I_M}{N_P} - \mu_P S_P, \tag{13}$$

$$\frac{dI_P}{dt} = \frac{\beta_P S_P I_M}{N_P} - (\gamma_P + \mu_P) I_P, \tag{14}$$

$$\frac{dR_P}{dt} = \gamma_P I_P - \mu_P R_P. \tag{15}$$

Mosquito Population

$$\frac{dS_M}{dt} = \Lambda_M - \frac{\beta_{MP} S_M I_P}{N_P} - \mu_M S_M, \tag{16}$$

$$\frac{dE_M}{dt} = \frac{\beta_{MP} S_M I_P}{N_P} - (\sigma_M + \mu_M) E_M, \tag{17}$$

$$\frac{dI_M}{dt} = \sigma_M E_M - \mu_M I_M, \tag{18}$$

with non-negative initial conditions, $N_H = S_H + V_H + E_H + I_H + R_H$, $N_P = S_P + I_P + R_P$, $N_M = S_M + E_M + I_M$. Define $k_H = \sigma_H + \mu_H$, $k_I = \gamma_H + \delta_H + \mu_H$, $k_P = \gamma_P + \mu_P$, $k_M = \sigma_M + \mu_M$.

System (8)–(18) is generalized to a fractional-order model using the Caputo derivative. The basis for choosing the operator, the derivation of the Volterra integral form, and the explicit substitution process are presented below.

Rationale for Choosing the Caputo Operator

Every equation in (8)–(18) takes the form $dx/dt = f(t, x)$, where the rate of change of compartment x at time t depends only on the current system state—a property called *Markovian* or locally time-dependent. In the JE epidemiological context this is not always realistic: the immune response to JEV is influenced by accumulated prior exposure [1, 16], and the extrinsic incubation period of *Culex* mosquitoes depends on accumulated ambient temperature over preceding days [17]. To accommodate such memory phenomena, d/dt must be generalized to a fractional derivative.

The Caputo operator is chosen over the Riemann–Liouville derivative for two reasons. First, Caputo initial conditions are expressed as integer-order derivative values, $x(0) = x_0$, measurable directly from surveillance data, whereas Riemann–Liouville requires fractional-integral initial conditions with no direct physical interpretation [12, 14]. Second, the Caputo derivative of a constant is zero, ${}^{C}D^{\alpha} c = 0$, ensuring consistency of the disease-free equilibrium E_0 between the ODE and fractional models [13]. Explicitly, for $\alpha \in (0, 1]$:

$${}^{C}D_t^{\alpha} x(t) = \frac{1}{\Gamma(1-\alpha)} \int_0^t (t-s)^{-\alpha} x'(s)\, ds, \tag{S.1}$$

where $\Gamma(\cdot)$ is the Euler Gamma function. The convolution kernel $(t-s)^{-\alpha}$ weights the entire history of $x'(s)$ from $s = 0$ to $s = t$, with the largest weight near $s = t$ decaying as a power-law—the long-range memory effect [14]. Smaller α implies slower weight decay and stronger past-to-present influence. When $\alpha \to 1$ the kernel becomes the Dirac delta $\delta(t-s)$ and (S.1) reduces to $x'(t)$, so the ODE model (8)–(18) is a special case with $\alpha = 1$ [13].

Derivation of the Volterra Integral Form

Consider the general fractional equation ${}^{C}D_t^{\alpha} x(t) = f(t, x(t))$. Applying the Caputo fractional integral $I^{\alpha}[g](t) = \frac{1}{\Gamma(\alpha)} \int_0^t (t-s)^{\alpha-1} g(s)\, ds$ to both sides and using the inverse property $I^{\alpha}({}^{C}D^{\alpha} x)(t) = x(t) - x(0)$ [13]:

$$x(t) = x(0) + \frac{1}{\Gamma(\alpha)} \int_0^t (t-s)^{\alpha-1} f(s, x(s))\, ds. \tag{S.4}$$

This Volterra representation underlies both the existence-uniqueness proof (Section 4.1) and the ABM discretization (Section 4.7). When $\alpha \to 1$, (S.4) reduces to the integral form of the ODE [13, 14].

Conversion from ODE System to Fractional Model

The generalization replaces every d/dt on the left-hand side with ${}^{C}D_t^{\alpha}$, while the right-hand side—encoding instantaneous biological mechanisms—remains unchanged. With commensurate order (Assumption 8), dimensional consistency is ensured [12]. Formally:

$$\frac{d}{dt}x_i(t) \;\longmapsto\; {}^{C}D_t^{\alpha}x_i(t) = \frac{1}{\Gamma(1-\alpha)}\int_0^t (t-s)^{-\alpha}x_i'(s)\,ds, \quad \alpha \in (0,1]. \tag{S.5}$$

For equation (8), the ODE for S_H becomes:

$${}^{C}D_t^{\alpha}S_H = \Lambda_H - \frac{\beta_H S_H I_M}{N_H} - (\phi_H + \mu_H)S_H, \tag{S.6}$$

which is equation (19). The recruitment term Λ_H and force of infection $\beta_H S_H I_M/N_H$ are unchanged since they represent instantaneous rates, but the overall dynamics of $S_H(t)$ now carry memory through kernel (S.5). Equations (9)–(12) convert identically:

$$\frac{dV_H}{dt} = \phi_H S_H - \mu_H V_H \quad\longmapsto\quad {}^{C}D_t^{\alpha}V_H = \phi_H S_H - \mu_H V_H, \quad (\to 20)$$

$$\frac{dE_H}{dt} = \frac{\beta_H S_H I_M}{N_H} - (\sigma_H + \mu_H)E_H \quad\longmapsto\quad {}^{C}D_t^{\alpha}E_H = \frac{\beta_H S_H I_M}{N_H} - (\sigma_H + \mu_H)E_H, \quad (\to 21)$$

$$\frac{dI_H}{dt} = \sigma_H E_H - (\gamma_H + \delta_H + \mu_H)I_H \quad\longmapsto\quad {}^{C}D_t^{\alpha}I_H = \sigma_H E_H - (\gamma_H + \delta_H + \mu_H)I_H, \quad (\to 22)$$

$$\frac{dR_H}{dt} = \gamma_H I_H - \mu_H R_H \quad\longmapsto\quad {}^{C}D_t^{\alpha}R_H = \gamma_H I_H - \mu_H R_H. \quad (\to 23)$$

For the pig population, equations (13)–(15) convert to:

$$\frac{dS_P}{dt} = \Lambda_P - \frac{\beta_P S_P I_M}{N_P} - \mu_P S_P \quad\longmapsto\quad {}^{C}D_t^{\alpha}S_P = \Lambda_P - \frac{\beta_P S_P I_M}{N_P} - \mu_P S_P, \quad (\to 24)$$

$$\frac{dI_P}{dt} = \frac{\beta_P S_P I_M}{N_P} - (\gamma_P + \mu_P)I_P \quad\longmapsto\quad {}^{C}D_t^{\alpha}I_P = \frac{\beta_P S_P I_M}{N_P} - (\gamma_P + \mu_P)I_P, \quad (\to 25)$$

$$\frac{dR_P}{dt} = \gamma_P I_P - \mu_P R_P \quad\longmapsto\quad {}^{C}D_t^{\alpha}R_P = \gamma_P I_P - \mu_P R_P. \quad (\to 26)$$

The term $\beta_P S_P I_M/N_P$ reflects pig infection by infectious mosquitoes, consistent with the amplifying host role (Assumption 3). The Caputo memory effect on I_P is biologically relevant since pig viremia is cyclical and shaped by prior JEV exposure history [18].

For the mosquito population, equations (16)–(18) convert to:

$$\frac{dS_M}{dt} = \Lambda_M - \frac{\beta_{MP} S_M I_P}{N_P} - \mu_M S_M \quad\longmapsto\quad {}^{C}D_t^{\alpha}S_M = \Lambda_M - \frac{\beta_{MP} S_M I_P}{N_P} - \mu_M S_M, \quad (\to 27)$$

$$\frac{dE_M}{dt} = \frac{\beta_{MP} S_M I_P}{N_P} - (\sigma_M + \mu_M)E_M \quad\longmapsto\quad {}^{C}D_t^{\alpha}E_M = \frac{\beta_{MP} S_M I_P}{N_P} - (\sigma_M + \mu_M)E_M, \quad (\to 28)$$

$$\frac{dI_M}{dt} = \sigma_M E_M - \mu_M I_M \quad\longmapsto\quad {}^{C}D_t^{\alpha}I_M = \sigma_M E_M - \mu_M I_M. \quad (\to 29)$$

The term $\beta_{MP} S_M I_P/N_P$ represents the rate at which susceptible mosquitoes become exposed via feeding on infectious pigs I_P, the primary JEV amplification pathway [16]. By Assumption 6 there is no recovery term in (29). The Caputo memory effect on E_M and I_M reflects the dependence of the mosquito extrinsic incubation period on accumulated environmental conditions [17, 13]. The resulting fractional model of order $\alpha \in (0, 1]$ is as follows.

Human Population (Fractional)

$$^{C}D_t^{\alpha} S_H = \Lambda_H - \frac{\beta_H S_H I_M}{N_H} - (\phi_H + \mu_H) S_H, \tag{19}$$

$$^{C}D_t^{\alpha} V_H = \phi_H S_H - \mu_H V_H, \tag{20}$$

$$^{C}D_t^{\alpha} E_H = \frac{\beta_H S_H I_M}{N_H} - (\sigma_H + \mu_H) E_H, \tag{21}$$

$$^{C}D_t^{\alpha} I_H = \sigma_H E_H - (\gamma_H + \delta_H + \mu_H) I_H, \tag{22}$$

$$^{C}D_t^{\alpha} R_H = \gamma_H I_H - \mu_H R_H. \tag{23}$$

Pig Population (Fractional)

$$^{C}D_t^{\alpha} S_P = \Lambda_P - \frac{\beta_P S_P I_M}{N_P} - \mu_P S_P, \tag{24}$$

$$^{C}D_t^{\alpha} I_P = \frac{\beta_P S_P I_M}{N_P} - (\gamma_P + \mu_P) I_P, \tag{25}$$

$$^{C}D_t^{\alpha} R_P = \gamma_P I_P - \mu_P R_P. \tag{26}$$

Mosquito Population (Fractional)

$$^{C}D_t^{\alpha} S_M = \Lambda_M - \frac{\beta_{MP} S_M I_P}{N_P} - \mu_M S_M, \tag{27}$$

$$^{C}D_t^{\alpha} E_M = \frac{\beta_{MP} S_M I_P}{N_P} - (\sigma_M + \mu_M) E_M, \tag{28}$$

$$^{C}D_t^{\alpha} I_M = \sigma_M E_M - \mu_M I_M. \tag{29}$$

Descriptions of variables and parameters are in Tables 1 and 2.

Table 1. Compartment descriptions for system (19)–(29).

Comp.	Description	Initial value	Source
S_H	Susceptible human	9,900	[19]
V_H	Vaccinated human	0	Assumption
E_H	Exposed human	30	[7]
I_H	Infectious human	70	[7]
R_H	Recovered human	0	Assumption
S_P	Susceptible pig	400	[18]
I_P	Infectious pig	600	[20]
R_P	Recovered/immune pig	0	Assumption
S_M	Susceptible mosquito	4,800	[13]
E_M	Exposed mosquito	100	[13]
I_M	Infectious mosquito	100	[13]

Table 2. Parameter descriptions for system (19)–(29).

Par.	Description	Value	Source
Λ_H	Human recruitment rate	$\mu_H N_H^*$	[19]
μ_H	Natural human death rate	$1/(70 \times 365)$	[19]
β_H	Mosquito→human transmission rate	0.30	[17]
ϕ_H	Human vaccination rate	0.01	[21]
σ_H	Intrinsic human incubation rate	0.10	[6, 7]
γ_H	Human recovery rate	0.10	[6, 7]
δ_H	JE-induced death rate	0.005	[6, 7]
Λ_P	Pig recruitment rate	$\mu_P N_P^*$	[22]
μ_P	Natural pig death rate	$1/(3 \times 365)$	[17]
β_P	Mosquito→pig transmission rate	0.50	[17]
γ_P	Pig recovery rate	0.14	[8]
Λ_M	Mosquito recruitment rate	$\mu_M N_M^*$	[13]
μ_M	Natural mosquito death rate	$1/14$	[13]
β_{MP}	Pig→mosquito transmission rate	0.40	[17]
σ_M	Extrinsic mosquito incubation rate	0.10	[17]
α	Caputo fractional order	$(0, 1]$	This study

4. Results and Discussion

4.1. Existence and Uniqueness of Solutions

System (19)–(29) can be written in Volterra integral form:

$$x_i(t) = x_i(0) + \frac{1}{\Gamma(\alpha)} \int_0^t (t-\xi)^{\alpha-1} K_i(\xi, x_i(\xi))\, d\xi, \quad i = 1, \ldots, 11. \tag{30}$$

Kernel K_1 (equation for S_H) satisfies the Lipschitz condition:

$$\|K_1(t, S_H) - K_1(t, \hat{S}_H)\| \leq \left(\frac{\beta_H \rho_{11}}{\varepsilon} + \phi_H + \mu_H\right) \|S_H - \hat{S}_H\|.$$

Let $c_1 = \beta_H \rho_{11}/\varepsilon + \phi_H + \mu_H$. Similarly, Lipschitz constants for K_i, $i = 2, \ldots, 11$:

$$\begin{aligned} &c_2 = \mu_H, \quad c_3 = k_H, \quad c_4 = k_I, \quad c_5 = \mu_H, \\ &c_6 = \beta_P \rho_{11}/\varepsilon + \mu_P, \quad c_7 = k_P, \quad c_8 = \mu_P, \\ &c_9 = \beta_{MP} \rho_7/\varepsilon + \mu_M, \quad c_{10} = k_M, \quad c_{11} = \mu_M, \end{aligned}$$

where $\varepsilon > 0$ is the lower bound of N_H, N_P, N_M on the feasible region Ω.

Constructing the recursive formula from (30):

$$G_{in}(t) = \frac{1}{\Gamma(\alpha)} \int_0^t (t-\xi)^{\alpha-1} (K_i(\xi, x_{i(n-1)}) - K_i(\xi, x_{i(n-2)}))\, d\xi,$$

the Lipschitz condition gives $\|G_{in}(t)\| \leq \|x_i(0)\| (c_i t/\Gamma(\alpha))^n$. A solution exists if $c_i t_1/\Gamma(\alpha) < 1$ for some $t_1 > 0$. Since $\lim_{n\to\infty} \|G_{in}(t)\| = 0$, the sequence x_{in} converges uniformly to the integral solution (30). Uniqueness follows by supposing two solutions exist: the Lipschitz condition gives $\|x_i - \hat{x}_i\| \leq (c_i t_1/\Gamma(\alpha))\|x_i - \hat{x}_i\|$, which forces $x_i = \hat{x}_i$ since $c_i t_1/\Gamma(\alpha) < 1$.

4.2. Positive Invariance on Ω

The feasible region is

$$\Omega = \{(S_H, \ldots, I_M) \in \mathbb{R}_+^{11} \mid N_H \le \tfrac{\Lambda_H}{\mu_H},\ N_P \le \tfrac{\Lambda_P}{\mu_P},\ N_M \le \tfrac{\Lambda_M}{\mu_M}\}. \tag{36}$$

By Lemma 1, ${}^{C}D_t^{\alpha} f(t_0) \ge 0$ implies f is non-decreasing near t_0. Evaluating each equation on the boundary of $\mathbb{R}_+^{11}$ confirms all boundary derivatives are non-negative, so $\mathbb{R}_+^{11}$ is positively invariant. Summing the human equations:

$${}^{C}D_t^{\alpha} N_H = \Lambda_H - \mu_H N_H - \delta_H I_H \le \Lambda_H - \mu_H N_H.$$

Via the Caputo Laplace transform and the Mittag–Leffler inverse:

$$N_H(t) \le \frac{\Lambda_H}{\mu_H} + E_\alpha(-\mu_H t^\alpha)\Big(N_H(0) - \frac{\Lambda_H}{\mu_H}\Big) \le \frac{\Lambda_H}{\mu_H}.$$

Identical arguments yield $N_P(t) \le \Lambda_P/\mu_P$ and $N_M(t) \le \Lambda_M/\mu_M$. Hence Ω is positively invariant and globally attracting.

4.3. Equilibrium Points

Equilibria are obtained by setting all fractional derivatives to zero.

Disease-free equilibrium (DFE). Setting $E_H = I_H = I_P = E_M = I_M = 0$:

$$E_0 = \Big(S_H^* = \tfrac{\Lambda_H}{\phi_H+\mu_H},\ V_H^* = \tfrac{\phi_H\Lambda_H}{\mu_H(\phi_H+\mu_H)},\ S_P^* = \tfrac{\Lambda_P}{\mu_P},\ S_M^* = \tfrac{\Lambda_M}{\mu_M},\ \text{others} = 0\Big). \tag{39}$$

Endemic equilibrium. When $\mathcal{R}_0 > 1$, a unique endemic equilibrium E^* with all positive components exists, where

$$I_P^* = \frac{\Lambda_P}{\mu_P + \gamma_P}\Big(1 - \frac{1}{\mathcal{R}_P}\Big), \quad I_M^* = \frac{\sigma_M}{\mu_M} E_M^*, \quad I_H^* = \frac{\sigma_H}{k_I} E_H^*.$$

4.4. Basic Reproduction Number

$\mathcal{R}_0$ is determined by the next-generation matrix method [23]. The infected compartments are $(E_H, I_H, I_P, E_M, I_M)^T$. The new infection matrix F and transfer matrix V at E_0 are:

$$F = \begin{pmatrix} 0 & 0 & 0 & 0 & \beta_H S_H^*/N_H^* \\ 0 & 0 & 0 & 0 & 0 \\ 0 & 0 & 0 & 0 & \beta_P S_P^*/N_P^* \\ 0 & 0 & \beta_{MP} S_M^*/N_P^* & 0 & 0 \\ 0 & 0 & 0 & 0 & 0 \end{pmatrix}, \quad V = \begin{pmatrix} k_H & 0 & 0 & 0 & 0 \\ -\sigma_H & k_I & 0 & 0 & 0 \\ 0 & 0 & k_P & 0 & 0 \\ 0 & 0 & 0 & k_M & 0 \\ 0 & 0 & 0 & -\sigma_M & \mu_M \end{pmatrix}.$$

Theorem 4.1. *The basic reproduction number of system (19)–(29) is*

$$\mathcal{R}_0 = \rho(FV^{-1}) = \sqrt{\frac{\beta_H \sigma_H}{k_H k_I} \cdot \frac{\mu_H}{\phi_H + \mu_H} \cdot \frac{\beta_{MP}\beta_P \sigma_M \Lambda_M}{\mu_M^2 k_P k_M \mu_P}}. \tag{43}$$

$\mathcal{R}_0$ does not depend on the fractional order α.

Proof. $K = FV^{-1}$ is computed analytically. K^2 has rank one since JEV transmission requires a two-link chain: infectious mosquito bites pig → pig infects new mosquito → new mosquito infects human. The unique nonzero eigenvalue of K^2 is $\lambda = \mathcal{R}_0^2$, giving $\mathcal{R}_0 = \sqrt{\lambda}$. Substituting $S_H^*/N_H^* = \mu_H/(\phi_H + \mu_H)$, $S_P^*/N_P^* = 1$, $S_M^*/N_P^* = \Lambda_M/(\mu_M N_P^*)$ yields (43). Independence from α follows because $\mathcal{R}_0$ is evaluated at the static equilibrium E_0, which contains no time-derivative terms. ∎

With parameter values from Table 2 and $N_P = 1000$, $N_M = 5000$, we obtain $\mathcal{R}_0 \approx 2.14 > 1$, consistent with the endemic condition in Bali.

4.5. Stability Analysis

Theorem 4.2 (Local Asymptotic Stability of the DFE)**.** *E_0 is locally asymptotically stable if $\mathcal{R}_0 < 1$ and unstable if $\mathcal{R}_0 > 1$.*

Proof. The Jacobian J_{E_0} has a lower block-triangular structure. The disease-free block yields negative real eigenvalues: $-(\phi_H + \mu_H)$, $-\mu_H$, $-\mu_P$, $-\mu_M$. The infected block's characteristic polynomial has all roots with negative real parts iff $\mathcal{R}_0 < 1$ (Routh–Hurwitz). For fractional systems with $\alpha \in (0, 1]$, stability requires $|\arg(\lambda_i)| > \alpha\pi/2$ (Matignon's criterion [24]). Since all eigenvalues are real and negative when $\mathcal{R}_0 < 1$, this is automatically satisfied for any $\alpha \in (0, 1]$. ∎

4.6. Sensitivity Analysis

The normalized forward sensitivity index [25] is

$$T_p^{\mathcal{R}_0} = \frac{\partial \mathcal{R}_0}{\partial p} \cdot \frac{p}{\mathcal{R}_0}. \tag{44}$$

A positive index means the parameter increases $\mathcal{R}_0$; a negative index means it decreases $\mathcal{R}_0$. Analytical indices from (43) are in Table 3.

Table 3. Sensitivity indices of $\mathcal{R}_0$ with respect to JE model parameters.

Par.	Description	Analytical expression	Value
β_{MP}	Pig→mosquito transmission rate	$+1/2$	+0.500
β_P	Mosquito→pig transmission rate	$+1/2$	+0.500
β_H	Mosquito→human transmission rate	$+1/2$	+0.500
σ_H	Intrinsic human incubation rate	$+\mu_H/[2(\sigma_H + \mu_H)]$	+0.499
σ_M	Extrinsic mosquito incubation rate	$+\mu_M/[2(\sigma_M + \mu_M)]$	+0.418
ϕ_H	Human vaccination rate	$-\phi_H/[2(\phi_H + \mu_H)]$	−0.478
γ_P	Pig recovery rate	$-\gamma_P/[2(\gamma_P + \mu_P)]$	−0.497
γ_H	Human recovery rate	$-\gamma_H/[2(\gamma_H + \delta_H + \mu_H)]$	−0.472
μ_M	Natural mosquito death rate	$-(3\mu_M + \sigma_M)/[2\mu_M(\sigma_M + \mu_M)]$	−1.418

The mosquito death rate μ_M has the largest absolute index (−1.418), indicating that vector control—larvicides in rice fields and insecticide spraying in pig farms—has the greatest impact on reducing $\mathcal{R}_0$. The pig-to-mosquito rate β_{MP} and mosquito-to-pig rate β_P (both +0.500) confirm the dominant role of the pig amplification cycle, consistent with the 96.6% pig seroprevalence in Bali [18]. The vaccination rate ϕ_H (index −0.478) confirms that expanding JE vaccination aligns with the 2023 IDAI recommendations [21].

4.7. Numerical Solution and Discussion

The numerical solution of (19)–(29) uses the predictor-corrector ABM scheme for fractional differential equations [26]. The Volterra form (30) is discretized on a uniform grid $t_k = kh$, $k = 0, 1, \ldots, m$, with $h = 1$ day.

Corrector formula:

$$x_{i,k+1} = x_i(0) + \frac{h^\alpha}{\Gamma(\alpha + 2)}\Big[\sum_{j=0}^{k} a_{j,k+1} K_i(t_j, x_{i,j}) + a_{k+1,k+1} K_i(t_{k+1}, x_{i,k+1}^P)\Big], \tag{45}$$

with weights

$$a_{j,k+1} = \begin{cases} k^{\alpha+1} - (k-\alpha)(k+1)^{\alpha}, & j = 0, \\ (k-j+2)^{\alpha+1} + (k-j)^{\alpha+1} - 2(k-j+1)^{\alpha+1}, & 1 \le j \le k, \\ 1, & j = k+1. \end{cases} \tag{46}$$

Predictor formula:

$$x^{p}_{i,k+1} = x_i(0) + \frac{h^{\alpha}}{\Gamma(\alpha+1)} \sum_{j=0}^{k} b_{j,k+1} K_i(t_j, x_{i,j}), \quad b_{j,k+1} = (k-j+1)^{\alpha} - (k-j)^{\alpha}. \tag{47}$$

Simulation is over $[0, 365]$ days using initial conditions from Table 1 and parameters from Table 2, for $\alpha \in \{1.00, 0.90, 0.85, 0.75\}$.

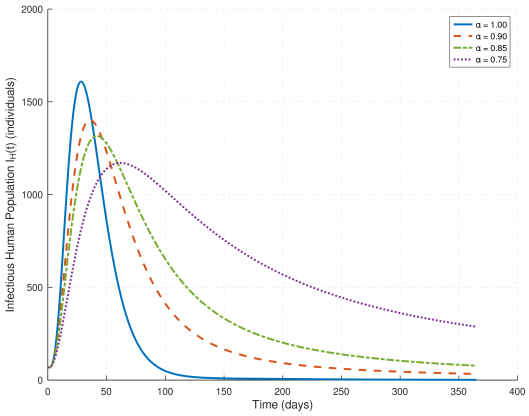


Figure 2. Compartment I_H (infectious human) for various fractional orders α.

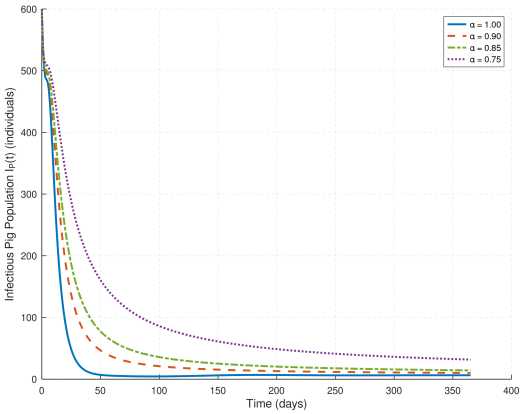


Figure 3. Compartment I_P (infectious pig) for various fractional orders α.

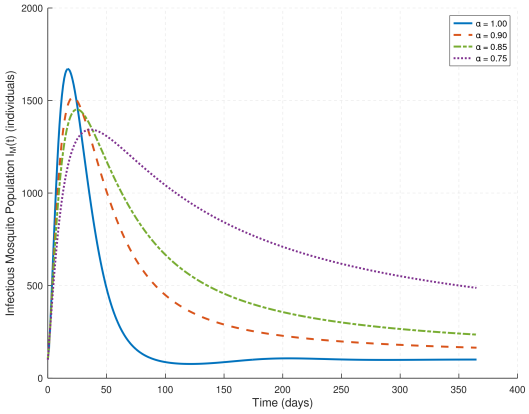


Figure 4. Compartment I_M (infectious mosquito) for various fractional orders α.

Figures 2–4 illustrate the influence of the fractional order α on the dynamics of Japanese encephalitis in the human, pig, and mosquito populations. In Figure 2, the infectious human population I_H reaches its highest peak under the integer-order model ($\alpha = 1.00$), approximately 1,600 individuals around day 30. As α decreases to 0.90 and 0.85, the peak becomes lower and occurs later, while for $\alpha = 0.75$ it produces a broader and substantially delayed peak of approximately 1,170 individuals around day 65. The post-peak trajectories also differ: the integer-order solution declines rapidly toward a very low level, whereas the fractional-order solutions exhibit more prolonged declines. Figure 3 shows a different pattern for the infectious pig population I_P. The trajectories decrease from their initial values under all four fractional orders, with the integer-order solution declining most rapidly. The fractional-order solutions decline more gradually, with lower values of α associated with greater persistence of infection. Figure 4 shows that the infectious mosquito population I_M exhibits a pronounced peak, reaching its highest peak under $\alpha = 1.00$ and progressively lower and later peaks as α decreases. Taken together, these results indicate that the Caputo derivative's history-dependent kernel alters the temporal distribution of infection. For human and mosquito infections, smaller α are associated with lower and later peaks, while for pig infections, the main difference is the persistence of infection over time.

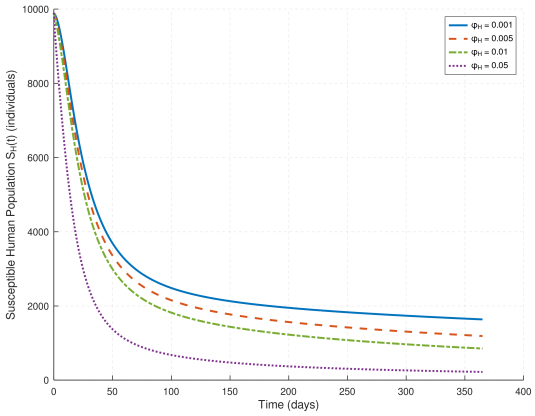


Figure 5. Effect of vaccination rate ϕ_H on compartment S_H.

Figure 5 illustrates the effect of the human vaccination rate ϕ_H on the susceptible human population S_H. Four vaccination rates are considered: $\phi_H = 0.001, 0.005, 0.01$, and 0.05. The

highest rate ($\phi_H = 0.05$) produces the fastest and most pronounced decline in S_H. This pattern is consistent with the susceptible-human equation,

$$^{C}D_t^{\alpha} S_H = \Lambda_H - \frac{\beta_H S_H I_M}{N_H} - (\phi_H + \mu_H) S_H,$$

in which the term $\phi_H S_H$ represents the transfer of susceptible individuals to the vaccinated compartment V_H. Increasing ϕ_H strengthens this transfer and therefore contributes directly to the reduction of the susceptible population. Under the model assumption that vaccinated individuals are fully protected from infection, this reduces the number of individuals remaining susceptible to mosquito-borne transmission. However, Figure 5 displays only the susceptible compartment, so the magnitude of any reduction in human exposure or infection cannot be determined from this figure alone.

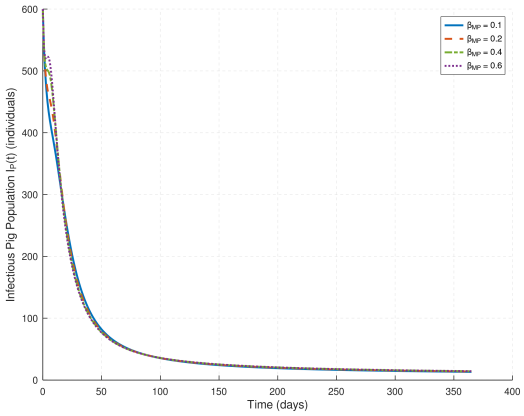


Figure 6. Effect of pig-to-mosquito transmission rate β_{MP} on compartment I_P.

Figure 6 illustrates the effect of the pig-to-mosquito transmission rate β_{MP} on the infectious pig population I_P. Four parameter values are considered: $\beta_{MP} = 0.1, 0.2, 0.4$, and 0.6. The results show that the four trajectories are closely overlapping throughout most of the simulation period. The parameter β_{MP} represents the transmission rate from infectious pigs to susceptible mosquitoes and appears directly in the mosquito infection term,

$$\frac{\beta_{MP} S_M I_P}{N_P}.$$

Its direct effect is on the rate at which susceptible mosquitoes become exposed through contact with infectious pigs. By contrast, β_{MP} does not appear directly in the differential equation for the infectious pig population I_P. Any influence on pig infection dynamics occurs indirectly through changes in the mosquito population and the subsequent mosquito-to-pig transmission pathway. Therefore, the overlapping trajectories should not be interpreted as evidence that β_{MP} has little influence on the overall transmission system; rather, the effect is compartment-specific. Further conclusions about the effect on mosquito infection dynamics would require the corresponding simulation results for E_M and I_M.

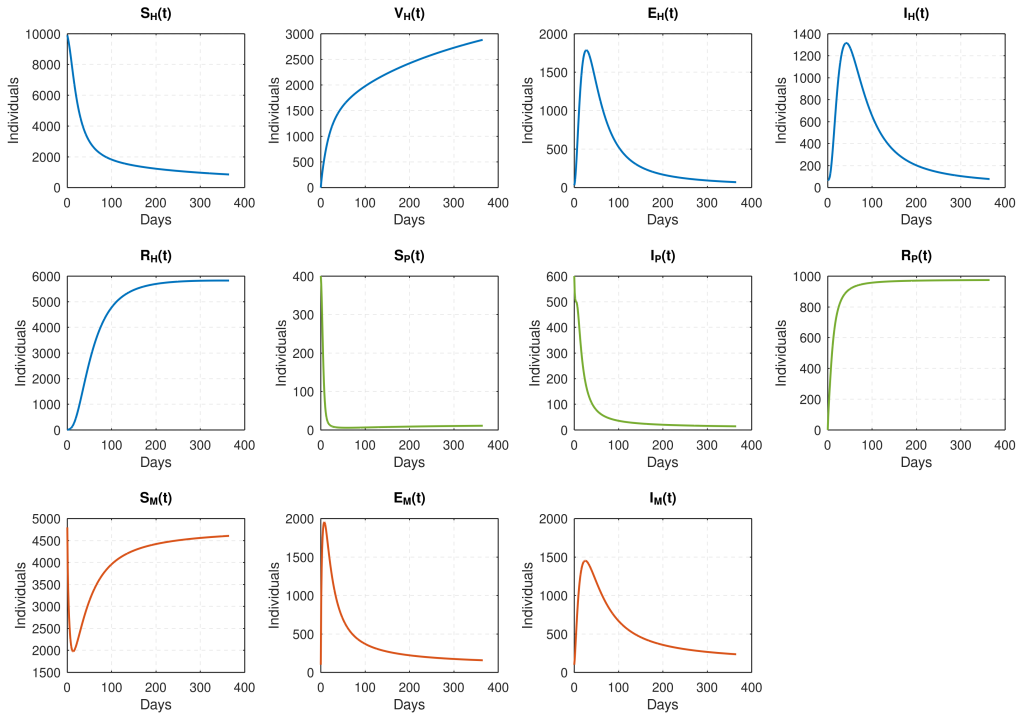


Figure 7. Dynamics of all compartments of the Caputo fractional JE model for $\alpha = 0.85$ with Bali initial conditions. Top row: human (S_H, V_H, E_H, I_H, R_H); middle row: pig (R_H, S_P, I_P, R_P); bottom row: mosquito (S_M, E_M, I_M).

Figure 7 shows the dynamics of all eleven compartments for $\alpha = 0.85$. The susceptible humans S_H decline rapidly, while the vaccinated V_H and recovered R_H populations increase. The exposed and infectious human populations peak and then decline, reflecting the progression of the disease. Similar patterns are observed for the pig and mosquito populations, illustrating the coupled transmission dynamics among the three species represented in the model.

4.8. Comparison with Previous Studies and Contributions

A direct comparison with Ghassabzade and Bagherpoorfard [11] is particularly relevant because their study also employed a Caputo fractional derivative for JE modeling. Their model includes seven principal state variables representing environmental discharge, an animal reservoir, aquatic mosquitoes, susceptible and infected mosquitoes, and human population states. In contrast, the present study uses eleven compartments. The two models therefore differ in their compartment structures and the biological processes represented. The two studies also employ different numerical approaches; Ghassabzade and Bagherpoorfard used a product-integration rule, whereas the present study uses the ABM predictor-corrector method.

The simulation results also provide a basis for comparison. Ghassabzade and Bagherpoorfard reported that decreasing the fractional order increased the infected human and mosquito populations in their simulations. In the present study, Figures 2 and 4 show a different pattern: decreasing the fractional order is associated with lower and later peaks. These differences indicate that the influence of the fractional order depends on the particular model structure, parameter values, initial conditions, and transmission mechanisms. The contribution of this study therefore lies not in the first application of fractional calculus to JE modelling, but in the specific combination of the eleven-compartment human-pig-mosquito structure, its mathematical analysis, and the investigation of fractional-order effects under the specified epidemiological

assumptions.

5. Conclusion

This study formulated and analysed an eleven-compartment Caputo fractional-order model of Japanese encephalitis (JE) transmission involving human, pig, and mosquito populations. The model incorporates human vaccination and disease progression, pig infection and recovery, and susceptible, exposed, and infectious mosquito compartments. Its mathematical properties were investigated through the analysis of solution existence and uniqueness, positive invariance, equilibrium points, the basic reproduction number, stability, and parameter sensitivity.

The numerical simulations using the Adams–Bashforth–Moulton predictor–corrector method demonstrate that the fractional order influences the temporal dynamics of infection across the three populations. For the simulated orders $\alpha \in \{1.00, 0.90, 0.85, 0.75\}$, decreasing α is associated with lower and later infection peaks in the human and mosquito populations, followed by more prolonged declines. In contrast, the infectious pig population exhibits a more gradual decline at lower fractional orders. As α approaches one, the fractional-order solutions converge towards the corresponding integer-order solution under the model formulation and simulation settings considered.

The parameter analyses further show that increasing the human vaccination rate accelerates the decline of the susceptible human population under the assumption of complete vaccine protection. Variations in the pig-to-mosquito transmission rate produce closely overlapping trajectories for the infectious pig population in the scenarios examined. This result is specific to the compartment displayed and does not establish the magnitude of the parameter's effect on mosquito infection dynamics, which requires examination of the corresponding mosquito compartments.

Compared with the fractional-order JE model of Ghassabzade and Bagherpoorfard [11], the present study provides a different compartmental formulation and investigates its numerical dynamics using the ABM predictor–corrector method rather than the product-integration approach. The contribution of this study therefore lies not in the first application of fractional calculus to JE modelling, but in the combination of the eleven-compartment human–pig–mosquito structure, its mathematical analysis, and the investigation of fractional-order effects under the specified epidemiological assumptions.

These findings characterize the mathematical behaviour of the proposed model under the selected parameter values and initial conditions. Because the simulations have not been validated against observed JE incidence data, the results should not be interpreted as evidence of superior predictive accuracy or as direct estimates of real-world transmission. Further work should examine the model against empirical data and investigate how alternative parameter values and epidemiological assumptions affect its predictions. Such extensions would help assess the practical relevance of the model for understanding JE transmission dynamics and evaluating potential control strategies.

References

[1] World Health Organization, "Japanese encephalitis," 2024. WHO Fact Sheets.

[2] G. W. Letson, A. A. Marfin, J. Mooney, H. V. Minh, and S. L. Hills, "Impact of vaccination against japanese encephalitis in endemic countries," *PLOS Neglected Tropical Diseases*, vol. 18, no. 9, p. e0012390, 2024.

[3] V. Baniya and R. Keval, "The influence of vaccination on the control of je with a standard incidence rate of mosquitoes, pigs and humans," *Journal of Applied Mathematics and Computing*, vol. 64, pp. 519–550, 2020.

[4] F. Ndaïrou, I. Area, and D. F. M. Torres, "Mathematical modeling of japanese encephalitis under aquatic environmental effects," *Mathematics*, vol. 8, no. 11, p. 1880, 2020.

[5] L. R. Sari, P. Andayani, and S. U. Wijaya, "Vector-reservoir transmission in a japanese encephalitis model," *Indonesian Journal of Mathematics and Applications*, vol. 1, no. 1, pp. 15–23, 2023.

[6] H. Ladreyt, V. Chevalier, and B. Durand, "Modelling japanese encephalitis virus transmission dynamics and human exposure in a cambodian rural multi-host system," *PLOS Neglected Tropical Diseases*, vol. 16, no. 7, p. e0010572, 2022.

[7] N. H. Tuan, H. Mohammadi, and S. Rezapour, "A mathematical model for covid-19 transmission by using the caputo fractional derivative," *Chaos, Solitons & Fractals*, vol. 140, p. 110107, 2020.

[8] M. F. Khan, H. Alrabaiah, S. Ullah, M. A. Khan, M. Farooq, M. Mamat, and M. I. Asjad, "A new fractional model for vector-host disease with saturated treatment function via singular and non-singular operators," *Alexandria Engineering Journal*, vol. 60, no. 1, pp. 629–645, 2021.

[9] S. O. Akindeinde, E. Okyere, A. O. Adewumi, R. S. Lebelo, O. O. Fabelurin, and S. E. Moore, "Caputo fractional-order seirp model for covid-19 pandemic," *Alexandria Engineering Journal*, vol. 61, no. 1, pp. 829–845, 2022.

[10] T. A. Laidlow *et al.*, "Scoping review of japanese encephalitis virus transmission models," *Transboundary and Emerging Diseases*, vol. 2025, p. 9880670, 2025.

[11] F. Akhavan-Ghassabzade and M. Bagherpoorfard, "Mathematical analysis of a novel japanese encephalitis fractional model," in *Proceedings of the 52nd Annual Iranian Mathematics Conference*, (Kerman, Iran), pp. 21–23, 2021.

[12] K. Diethelm, *The Analysis of Fractional Differential Equations: An Application-Oriented Exposition Using Differential Operators of Caputo Type*, vol. 2004 of *Lecture Notes in Mathematics*. Berlin: Springer, 2010.

[13] I. Podlubny, *Fractional Differential Equations*. San Diego: Academic Press, 1999.

[14] A. A. Kilbas, H. M. Srivastava, and J. J. Trujillo, *Theory and Applications of Fractional Differential Equations*. Amsterdam: Elsevier, 2006.

[15] Z. M. Odibat and N. T. Shawagfeh, "Generalized taylor's formula," *Applied Mathematics and Computation*, vol. 186, no. 1, pp. 286–293, 2007.

[16] T. E. Erlanger, S. Weiss, J. Keiser, J. Utzinger, and K. Wiedenmayer, "Past, present, and future of japanese encephalitis," *Emerging Infectious Diseases*, vol. 15, no. 1, pp. 1–7, 2009.

[17] I. M. Kardena, A. A. A. M. Adi, I. N. M. Astawa, M. O'Dea, M. Laurence, S. Sahabizada, and M. Bruce, "Japanese encephalitis in bali, indonesia: ecological and socio-cultural perspectives," *International Journal of Environmental Research and Public Health*, vol. 20, no. 1, p. 31, 2023.

[18] I. M. Kardena, A. A. A. M. Adi, I. N. M. Astawa, S. Sahabizada, M. Bruce, and M. O'Dea, "Individual and herd-level seroprevalence in association with potential risk factors of japanese encephalitis in pigs collected from urban, periurban, and rural areas of indonesia," *Veterinary Medicine International*, vol. 2023, p. 9682657, 2023.

[19] Badan Pusat Statistik, "Statistik indonesia 2023," 2023.

[20] K. Kari, W. Liu, K. Gautama, M. P. Mammen, J. D. Clemens, A. Kisdi, K. Subrata, H. K. Kim, and Z. Y. Xu, "A hospital-based surveillance for japanese encephalitis in bali, indonesia," *BMC Medicine*, vol. 7, p. 6, 2009.

[21] Kementerian Kesehatan Republik Indonesia, "Program imunisasi japanese encephalitis," 2023.

[22] Badan Pusat Statistik Provinsi Bali, "Bali dalam angka 2023," 2023.

[23] P. van den Driessche and J. Watmough, "Reproduction numbers and sub-threshold endemic equilibria for compartmental models of disease transmission," *Mathematical Biosciences*, vol. 180, pp. 29–48, 2002.

[24] D. Matignon, "Stability results for fractional differential equations with applications to control processing," in *Computational Engineering in Systems Applications*, vol. 2, pp. 963–968, 1996.

[25] N. Chitnis, J. M. Hyman, and J. M. Cushing, "Determining important parameters in the spread of malaria through the sensitivity analysis of a mathematical model," *Bulletin of Mathematical Biology*, vol. 70, no. 5, pp. 1272–1296, 2008.

[26] K. Diethelm, N. J. Ford, and A. D. Freed, "A predictor-corrector approach for the numerical solution of fractional differential equations," *Nonlinear Dynamics*, vol. 29, pp. 3–22, 2002.